CDDpress

www.nature.com/cddis

ARTICLE OPEN

# Impaired BDNF-TrkB trafficking and signalling in Down syndrome basal forebrain neurons

Emily Blackburn[1,2,4], Nicol Birsa[1], André Teixeira Lopes[1], Elizabeth M. C. Fisher[1], Oscar M. Lazo[1,2,3] and Giampietro Schiavo[1,2]✉

© The Author(s) 2026

Brain derived neurotrophic factor (BDNF) and its receptor tropomyosin-related kinase B (TrkB) play crucial roles in neuronal development, synaptic transmission, and neuroplasticity. Deficits in BDNF/TrkB signalling and trafficking have been identified in several neurodegenerative diseases, including Alzheimer's disease (AD). Individuals with Down syndrome (DS) are at an increased risk of developing AD compared to the general population. Basal forebrain neurons (BFNs) are among the first to degenerate in AD and DS, but the mechanisms underlying their vulnerability remain unclear. Using BFNs derived from the Dp1Tyb mouse model of DS, we investigated neurotrophic signalling and trafficking deficits in AD-DS. We found enlarged early endosomes and elevated levels of active Rab5, a GTPase critical for early endosome formation, in Dp1Tyb BFNs. These abnormalities were associated with impaired transport of internalised TrkB from axon terminals to the soma. Using microfluidic devices, we demonstrated that axonal BDNF stimulation enhanced signalling endosome dynamics in wild-type but not Dp1Tyb BFNs, which is likely due to impaired axonal ERK1/2 signalling. Our findings establish a link between Rab5 hyperactivation, endosomal dysfunction, and impaired ERK1/2 signalling, highlighting the interplay between trafficking and neurotrophic signalling, and underscore the importance of targeting endolysosomal and signalling pathways to mitigate neuronal dysfunction in AD-DS.

*Cell Death and Disease* (2026)17:214 ; https://doi.org/10.1038/s41419-026-08464-z

## INTRODUCTION

Neurotrophic signalling is crucial for the differentiation, growth and survival of neurons, as well as synaptic transmission and neuroplasticity. Neurotrophins, namely nerve growth factor (NGF), brain-derived neurotrophic factor (BDNF), neurotrophic factor-3 (NT-3) and neurotrophic factor 4 (NT-4), are a family of structurally related proteins that bind with high affinity to specific tyrosine kinase receptors (TrkA-C) [1]. Following expression and secretion from target tissues, neurotrophins bind to Trk receptors mainly at axon terminals, activating the phosphoinositide 3-kinase (PI3K)-Akt, mitogen-activated protein kinase (MAPK-ERK) and phospholipase C-gamma (PLCγ) signalling pathways [1]. All four neurotrophins also bind the p75 neurotrophin receptor ($p75^{NTR}$), which interacts with Trk receptors, modulating their function [2].

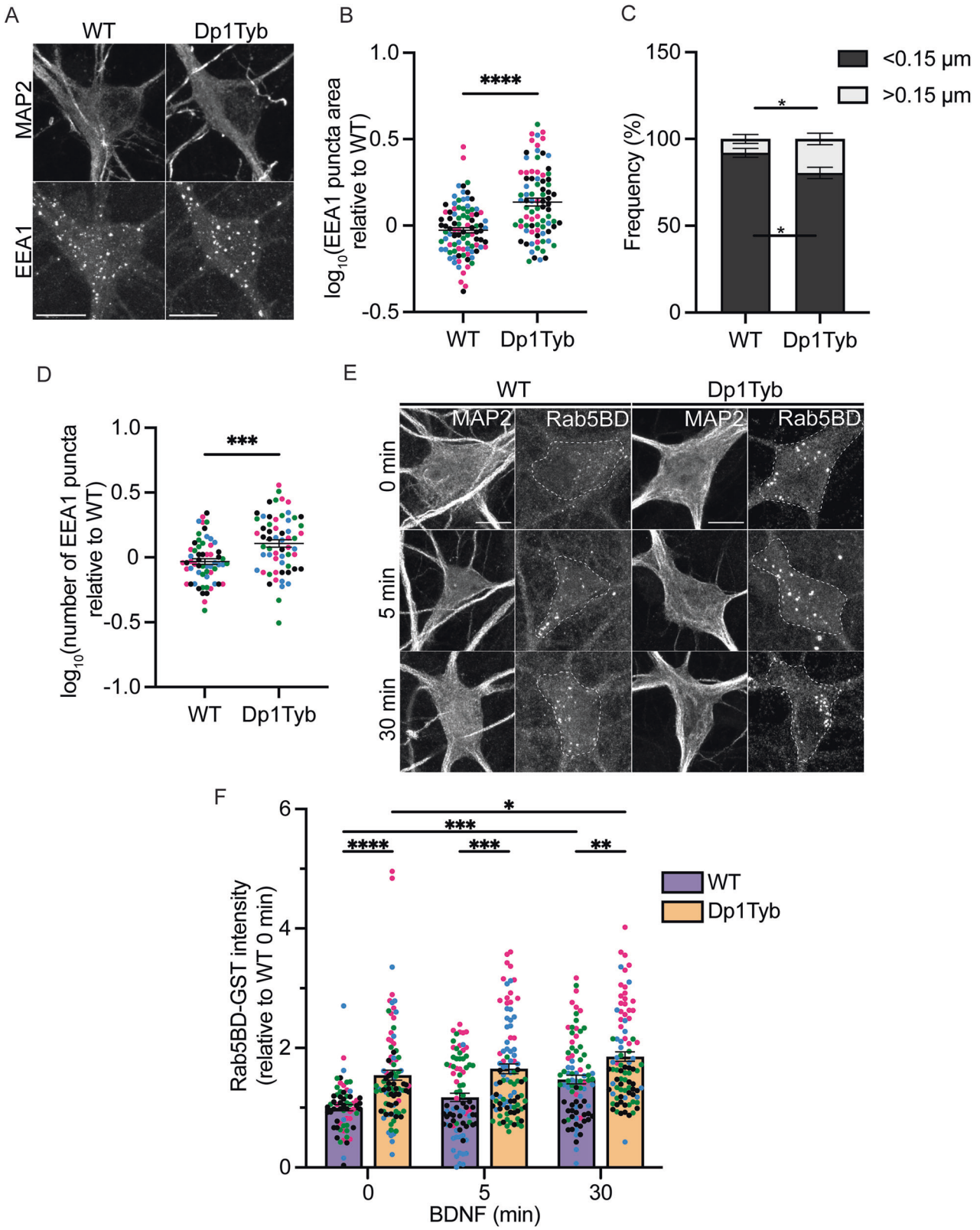
Neurotrophic signalling promotes both local and long-distance effects in neurons; at nerve terminals, it enables axonal branching and elongation, as well as synapse maturation and plasticity [3–5]. Distal action requires the propagation of signals regulating gene expression, survival, development and dendritic arborisation to the cell body via the axonal retrograde transport of activated neurotrophin-Trk complexes [5–8]. This transport is mediated by the recruitment of cytoplasmic dynein onto signalling endosomes [9–11], highlighting a critical relationship between axonal retrograde transport and long-distance propagation of neurotrophic signals. The internalisation of activated neurotrophin-Trk complexes from the plasma membrane, and the subsequent formation and maturation of these organelles, is regulated by Rab proteins - monomeric GTPases that cycle between an active, GTP-bound, membrane-associated state and an inactive GDP-bound cytosolic form [12].

Following internalisation, activated neurotrophin-Trk complexes are targeted to early endosomes which are regulated by Rab5, a GTPase crucial for receptor sorting and homotypic fusion of these organelles, among other functions [13]. The complex is then returned to the plasma membrane via Rab4/11 recycling endosomes or sorted to Rab7-positive late endosomes for delivery to the soma, or to lysosomes for degradation [14, 15]. In primary neurons, following activation by BDNF, TrkB has been shown to localise to both Rab5 and Rab11 positive compartments in dendrites and the cell body, a process crucial for dendritic branching [16, 17]. ERK1/2-dependent CREB phosphorylation in the nucleus also depends on both Rab5 and Rab11 [18] as well as Rab10 [19]. Upon BDNF treatment, Rab10-positive compartments are mobilised towards axon terminals, facilitating the sorting of TrkB into the axonal retrograde transport pathway [19]. Thus, the precise spatial and temporal association of Trk receptors with specific Rab membrane compartments is crucial for the coordination between local effects and

[1]Department of Neuromuscular Diseases and UCL Queen Square Motor Neuron Disease Centre, UCL Queen Square Institute of Neurology, University College London, London, UK. [2]UK Dementia Research Institute at UCL, University College London, London, UK. [3]Facultad de Psicología y Humanidades, Universidad San Sebastián, Santiago, Chile. [4]Present address: The Francis Crick Institute, London, UK. ✉email: giampietro.schiavo@ucl.ac.uk

Edited by Gerry Melino

Received: 15 July 2025 Revised: 13 December 2025 Accepted: 30 January 2026
Published online: 11 February 2026




long-distance propagation of neurotrophic signalling in neurons.

Deficits in signalling and trafficking of neurotrophic receptors have been identified in many neurodegenerative diseases [20, 21]. For example, disrupted axonal transport is an early event in Alzheimer's disease (AD), occurring prior to the formation of Aβ plaques and neurofibrillary tangles in familial AD mouse models [22–24]. Trisomy of chromosome 21 (Chr21), which gives rise to Down syndrome (DS), is the most common genetic cause of AD (referred to as AD-DS), with most individuals having AD-like

**Fig. 1 Early endosomes are enlarged and display increased Rab5 activity in basal forebrain neurons isolated from Dp1Tyb embryos.** **A** Representative confocal images of EEA1 immunofluorescence in WT and Dp1Tyb BFNs at DIV14. **B** EEA1 positive puncta were significantly larger in Dp1Tyb neurons compared to WT (Student's *t* test; ****$p < 0.0001$). **C** The size distribution of EEA1 positive puncta in Dp1Tyb BFNs showed a significant shift from smaller to larger binned areas compared to WT littermates (Student's *t* test; *$p = 0.0320$). **D** Quantification of EEA1 puncta number in Dp1Tyb BFNs compared to WT (Student's t-test; ***$p = 0.0002$). **E** Representative images of WT and Dp1Tyb neurons incubated with GST-Rab5BD to measure levels of GTP- Rab5 in the cell bodies (dashed lines) following 0, 5, 30 min BDNF treatment. **F** BDNF significantly increased GTP bound Rab5 in BFNs after 30 min treatment. GTP-Rab5 levels were significantly elevated in Dp1Tyb BFNs compared to WT at baseline and with BDNF treatment. (2-way ANOVA with Tukey's multiple comparisons; BDNF; ****$p < 0.0001$, genotype; ****$p < 0.0001$. Multiple comparisons; ****$p < 0.0001$, ***$p = 0.0009$, **$p = 0.0072$, *$p = 0.0368$). Different coloured points represent cells from separate *N*s. Bars represent mean ± SEM. $N = 4$ biological replicates. 15–25 cells were imaged per *N*. Scale bar = 10 µm.

neuropathology by the age of 40 [25]. The key dosage-sensitive Chr21 gene underpinning the increased risk of AD is the *APP* gene, which encodes the amyloid precursor protein; however, several other proteins encoded by genes on Chr21 have also been suggested to play a role in AD-DS [26]. Notably, the cholinergic system is particularly vulnerable in both DS and AD, as cholinergic basal forebrain neurons (BFNs) rely heavily on the retrograde transport of neurotrophins to maintain their cholinergic identity [27, 28].

Several studies have found abnormalities in neurotrophin signalling in AD and AD-DS, including reduced neurotrophin and Trk receptor levels [29, 30] impaired neurotrophin transport [31–34] and deficits in BDNF-related signalling via ERK and AKT [34]. Furthermore, impaired endosome morphology and function are early events in AD and DS human *post-mortem* tissue and mouse models [34–44]. It has been suggested that APP, and its associated ß-secretase cleaved, membrane-bound carboxy terminal fragment (ß-CTF), induce this pathological phenotype via Rab5 hyperactivation [39, 42, 44–46]. Additionally, enlarged endosomes convey trophic signals less effectively both in vitro and in vivo [32, 43]. Thus, the available evidence suggests that defects in neurotrophic signalling are not only directly related to neurotrophin/Trk levels but also implicate impaired axonal retrograde trafficking of signalling endosomes in AD and DS.

Here, we use an established model of DS, the Dp1Tyb mouse, which has an extra copy of the human Chr21 (Hsa21) orthologous genes on mouse chromosome 16 (Mmu16), comprising 63% of all Hsa21-orthologous mouse genes [47, 48]. However, most research exploring the role of early endosomes and neurotrophic signalling in the pathogenesis of AD-DS has been conducted using the Ts65Dn mouse. This mouse carries 60 annotated genes that are not homologous to Hsa21. Included in this group are at least four genes (*Snx9*, *Synj2*, *Dynlt1*, *Sylt3*) encoding proteins involved in the endocytic pathway and/or vesicular trafficking [49]. Indeed, many of these genes could contribute to Ts65Dn phenotypes and act as confounding factors in the analysis of the pathomechanism of AD-DS.

The aim of this work was to address whether BFNs, a highly vulnerable neuronal population in DS and in AD, isolated from Dp1Tyb embryos display neurotrophic signalling and trafficking deficits. We confirmed the presence of enlarged early endosomes in BFNs and identified increased levels of active Rab5 specifically in Dp1Tyb neurons. Furthermore, we found that BDNF enhances the transport dynamics of BDNF/TrkB signalling endosomes in WT but not Dp1Tyb BFNs, which is likely due to impaired ERK1/2 signalling in Dp1Tyb BFN axons.

## RESULTS

### Early endosome morphology and function are altered in Dp1Tyb basal forebrain neurons

To identify whether BFNs derived from Dp1Tyb mice display early endosome abnormalities, we stained DIV14 neurons for EEA1, an established early endosomal marker (Fig. 1A). Dp1Tyb BFNs displayed significantly enlarged early endosomes, >50% larger than those seen in WT BFNs (Fig. 1B). Furthermore, there was a ~60% increase in the number of larger endosomes and a ~13% reduction in the number of smaller endosomes in Dp1Tyb neurons (Fig. 1C). Early endosomes were also more numerous in Dp1Tyb BFNs (Fig. 1D).

It has been suggested that Rab5 hyperactivation underpins the early endosomal enlargement in AD and AD-DS [50]. As such, we wanted to ascertain whether there were increased levels of active Rab5 in Dp1Tyb BFNs. We used an in-situ approach using GST-fused to the Rab5 binding domain of Rabaptin-5 (Rab5BD) as a probe to specifically measure GTP-bound endogenous Rab5 (Rab5-GTP), followed by an immunostaining against GST (Fig. 1E). Rabaptin5 is a Rab5 effector that preferentially binds active Rab5 [51]. Prior to incubating with the Rab5BD probe, BFNs were treated with BDNF for 0, 5 or 30 min to determine whether BDNF stimulation induces an increase in Rab5 activity, as has been previously shown in primary hippocampal neurons [17].

We found that in WT neurons there was a significant increase in Rab5-GTP after 30 min BDNF treatment, confirming that BDNF increases Rab5 activity. Consistent with the increased size of early endosomes, Dp1Tyb BFNs already showed significantly higher levels of Rab5-GTP at baseline (0 min); these are comparable to those found in stimulated WT neurons, indicating increased basal levels of active Rab5 (Fig. 1F). Interestingly, when we looked at the total levels of Rab5 in axons, although the mean expression levels did not significantly differ between genotypes, the data display a much higher dispersion in Dp1Tyb neurons compared to WT, which is compatible with Rab5 heterogeneously clustering in different segments of each axon (Supplementary Fig. 1A, B).

As positive and negative controls for Rab5-GTP experiments, we incubated SH-SY5Y neuroblastoma cells transfected with constitutively active (Rab5CA) or dominant-negative Rab5 (Rab5DN) mutants, with the GST-Rab5BD probe (Supplementary Fig. 1C, E). Cells were also incubated with GST alone to rule out non-specific GST binding (Supplementary Fig. 1D). Early biochemical studies indicate that the N133I mutant acts as a dominant-negative through poor prenylation and membrane binding [52]. Thus, whilst it is expected to bind GST-Rab5BD, the lack of a punctate binding pattern further indicates the specificity of our assay.

Altogether, these results highlight that Dp1Tyb BFNs exhibit elevated baseline levels of Rab5-GTP resembling WT neurons treated with BDNF, indicating an inherent increase in Rab5 activity in these neurons compared to WT controls.

### The BDNF-dependent enhancement of axonal transport of signalling endosomes is impaired in Dp1Tyb BFNs

Next, we wanted to investigate whether increased levels of active Rab5 and enlargement of early endosomes impacted the axonal trafficking of BDNF-TrkB complexes. To test this hypothesis, we first determined whether WT and Dp1Tyb BFNs display differences in TrkB levels. As shown in Supplementary Fig. 2A, B, although the expression of TrkB is developmentally regulated in BFNs, we found no differences between the two genotypes at each timepoint. To exclude the possibility that membrane distribution of TrkB influenced our analysis, we performed immunostaining under non-permeabilizing conditions to label only surface TrkB. Consistently, surface TrkB levels did not differ between genotypes (Supplementary Fig. 2C, D).

While effective for detecting total TrkB expression, immunofluorescence quantification does not distinguish between the different isoforms of this receptor. Thus, we used western blotting to differentiate between full length TrkB (TrkB-FL) and its truncated T1 isoform (TrkB-T1); however, our analysis revealed no significant difference in TrkB-FL, TrkB-T1 levels, or the FL/T1 ratio (Supplementary Fig. 2E, F).

To evaluate the axonal retrograde transport of BDNF-TrkB complexes in live neurons, we exploited the non-toxic binding fragment of tetanus neurotoxin bound to AlexaFluor-555 ($H_CT$-555). $H_CT$ has been shown to share axonal retrograde transport carriers with neurotrophins and their receptors and is a reliable proxy of BDNF-TrkB signalling endosome dynamics [13, 53, 54]. We first confirmed $H_CT$/TrkB colocalization in BFNs. As expected, the number of TrkB, $H_CT$ and TrkB/$H_CT$ axonal carriers significantly increased with BDNF treatment (Supplementary Fig. 3A, B). Next, to facilitate axonal transport analysis, primary BFNs were grown in three-chamber microfluidic chambers (MFCs; Fig. 2A). These devices allow cellular and fluidic isolation of axon terminals, whilst also reducing variability between different dishes through the projection of axons from the same pool of neurons into two fluidically-isolated compartments. DIV14 BFNs were starved of growth factors and axonal compartments were then supplemented with $H_cT$-555 in the presence or absence of 50 ng/mL BDNF 30 min prior to imaging and tracking.

Under basal conditions, WT and Dp1Tyb BFCNs display average signalling endosome transport speeds and percentage of pausing that were comparable (~1.5 µm/s and ~29%, respectively). BDNF significantly increased the average velocity of retrograde signalling endosomes in WT BFNs (~30%; Fig. 2B, F) and significantly reduced pausing (>50%; Fig. 2D). However, in Dp1Tyb BFNs, BDNF treatment did not enhance transport speeds (Fig. 2C, G) or reduce pausing (Fig. 2E). Further analysis per axon emphasised these findings (Supplementary Fig. 3C, D). BDNF did not significantly alter the number of motile signalling endosomes in either genotype (Supplementary Fig. 3E, F). Given the established role of Rab7 in fast axonal retrograde transport[13], we also analysed the levels of total Rab7 in WT and Dp1Tyb BFNs, however we found no significant difference between the two genotypes (Supplementary Fig. 3G, H).

### Impaired retrograde TrkB trafficking in Dp1Tyb basal forebrain neurons

To assess whether axonal transport abnormalities translate into a deficit in the somatic transfer of internalised TrkB from axon terminals, we used a retrograde accumulation assay previously optimised by our group [19]. Twenty-four hours prior to the experiment, the axons of BFNs grown in three-chamber MFCs were incubated with the lipophilic tracers DiI or DiO to identify which neurons had axons projecting into the two axonal compartments. BFNs were then depleted of endogenous growth factors for 2 h prior to supplementing axonal compartments with anti-TrkB antibodies followed by 50 ng/mL BDNF or an anti-BDNF blocking antibody (Fig. 3A). Immunofluorescence staining of the somatic compartments after 2.5 h revealed TrkB antibodies in the soma of neurons stimulated with BDNF, but not in neurons depleted of BDNF via a blocking antibody (Fig. 3B). Dp1Tyb BFNs displayed a 30% reduction in the accumulation of TrkB compared to WT BFNs, suggesting reduced axonal retrograde transport of TrkB (Fig. 3C–E).

### BDNF signalling is impaired in Dp1Tyb basal forebrain neurons

Next, we wanted to determine whether the signalling pathways downstream of TrkB activation by BDNF were impaired in Dp1Tyb BFNs. Activation of the PI3K-AKT and MAPK-ERK1/2 pathways are crucial for neuronal survival, and alterations in their signalling have been reported in AD-DS models [34]. To test these signalling cascades in our system, BFNs were depleted of endogenous growth factors prior to stimulating with 50 ng/mL BDNF for 0, 30, or 120 min and immunostaining for pERK1/2 and pAKT(S473). MAP2 was used as a mask to measure the activation of these signalling cascades within the somatodendritic compartment.

The activation of ERK1/2 appeared significantly impaired in Dp1Tyb BFNs, with a reduction in the amplitude of BDNF response between the two genotypes at 30 min (Fig. 4A, B). In contrast, this approach did not allow us to detect the effect of BDNF on the activation of pAKT(S473) in either genotype (Supplementary Fig. 4A, B), likely due to high basal signal.

Interestingly, these findings do not align with our preliminary data using whole cell lysates probed by western blot (Supplementary Fig. 4C), which suggested impaired AKT activation in Dp1Tyb cultures (Supplementary Fig. 4D), and lack of effect of genotype on pERK1/2 levels (Supplementary Fig. 4E). However, a close inspection of these cultures suggests that the discrepancies in ERK1/2 activation between immunofluorescence and western blot datasets is likely due to differences in the number, and/or activation response of glial cells within the WT and Dp1Tyb BFN cultures. Indeed, we observed increased pERK1/2 staining in non-neuronal cells in Dp1Tyb cultures compared to WT, which further increased upon BDNF treatment, suggesting ERK1/2 activation in these cells is TrkB-dependent (Supplementary Fig. 4F, G). These apparently conflicting results highlight the importance of neuron-specific analyses when studying signalling pathways in the context of AD-DS and warrants further investigation.

Given the axonal transport impairment identified above, and the strong link between BDNF-induced ERK1/2 activation and axonal transport [55, 56], we next investigated the activation of ERK1/2 specifically in axons by immunofluorescence. BFNs grown in three-chamber MFCs were depleted of endogenous growth factors prior to treating axons with 50 ng/mL BDNF for 5 min. Whilst treatment for 5 min with BDNF significantly increased the levels of activated ERK1/2 in the axon of WT BFNs (Fig. 4C–E), there was no significant increase in ERK1/2 activation in Dp1Tyb BFNs (Fig. 4C, D, F), suggesting impaired axonal ERK1/2 signalling.

### ERK1/2 inhibition in WT neurons mimics the axonal transport impairment identified in Dp1Tyb neurons

To understand whether impaired ERK1/2 activation was contributing to the BDNF-TrkB transport impairment, we treated axons of BFNs cultured in three-chamber MFCs with BDNF ± ERK1/2 inhibitor U0126 (Fig. 5A). This inhibitor is effective in blocking the activation of ERK1/2 in both WT and Dp1Tyb BFNs as shown in cell lysates by western blot (Supplementary Fig. 5). We found that impairing ERK1/2 activation by treatment with U0126 caused a 25% reduction in the average axonal transport velocity of signalling endosomes in WT BFNs (Fig. 5B, C, G). Moreover, U0126 resulted in a 3.4-fold increase in the pausing of signalling endosomes in WT axons (Fig. 5E), suggesting that the effect of BDNF on the axonal retrograde transport of signalling endosomes requires ERK1/2 activation. In contrast, the ERK1/2 inhibitor had no effect on the axonal retrograde transport of signalling endosomes in Dp1Tyb BFNs (Fig. 5D, F, H), reflecting the limited ERK1/2 activation by BDNF in these Dp1Tyb neurons.

## DISCUSSION

Our results identify altered endosomal dynamics and impaired BDNF/TrkB trafficking in Dp1Tyb BFNs, concomitant with decreased ERK1/2 signalling in the axon, a result with potential implications for understanding neurodegenerative processes in AD-DS. We suggest that enlarged early endosomes underpin impaired ERK1/2 signalling, leading to compromised transport of signalling endosomes. Both local and long-distance neurotrophic signalling are crucial for neuronal survival and maintenance. Since physiological growth factor signalling requires functional

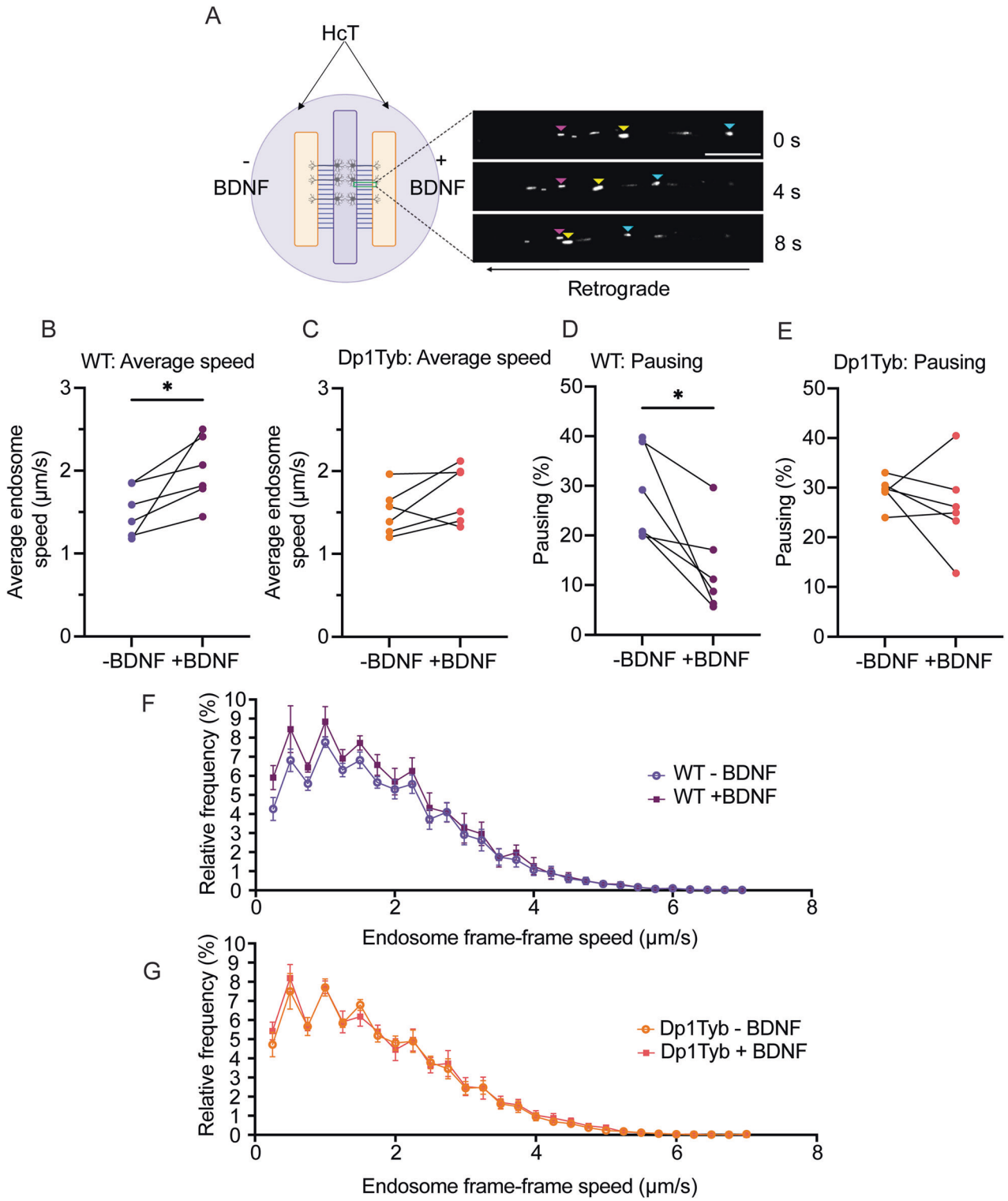



**Fig. 2 BDNF enhancement of signalling endosome transport is impaired in Dp1Tyb basal forebrain neurons. A** Schematic of the three-chamber MFC used to culture primary BFNs for axonal transport experiments. Axonal compartments were incubated with Alexafluor555-HcT (HcT-555) ± BDNF and time-lapse imaging was conducted within the MFC microgrooves. Endosomes were manually tracked using TrackMate. Pink arrows highlight a paused endosome, yellow/cyan arrows highlight retrogradely moving endosomes. Scale bar = 20 µm. **B**, **C** Average endosome speed in WT and Dp1Tyb BFNs in response to BDNF. Lines represent paired conditions within the same three-chambers MFC. BDNF significantly enhances signalling endosome speed in WT (paired Student's *t* test; $*p = 0.0372$), but not in Dp1Tyb (paired Student's *t* test; $p = 0.1462$) BFNs. **D**, **E** Percentage of pausing of HcT-555-positive signalling endosomes in response to BDNF. BDNF significantly reduces the percentage of pausing in WT (paired Student's *t* test; $*p = 0.0186$), but not Dp1Tyb (paired Student's *t* test; $p = 0.4451$) primary BFNs. **F**, **G** Speed distribution curves of signalling endosome transport in WT and Dp1Tyb neurons ± BDNF. Endosome pausing (speed <0.25 µm/s) was excluded from the curves). All graphs $N = 6$ biological replicates, 5–8 axons per condition.

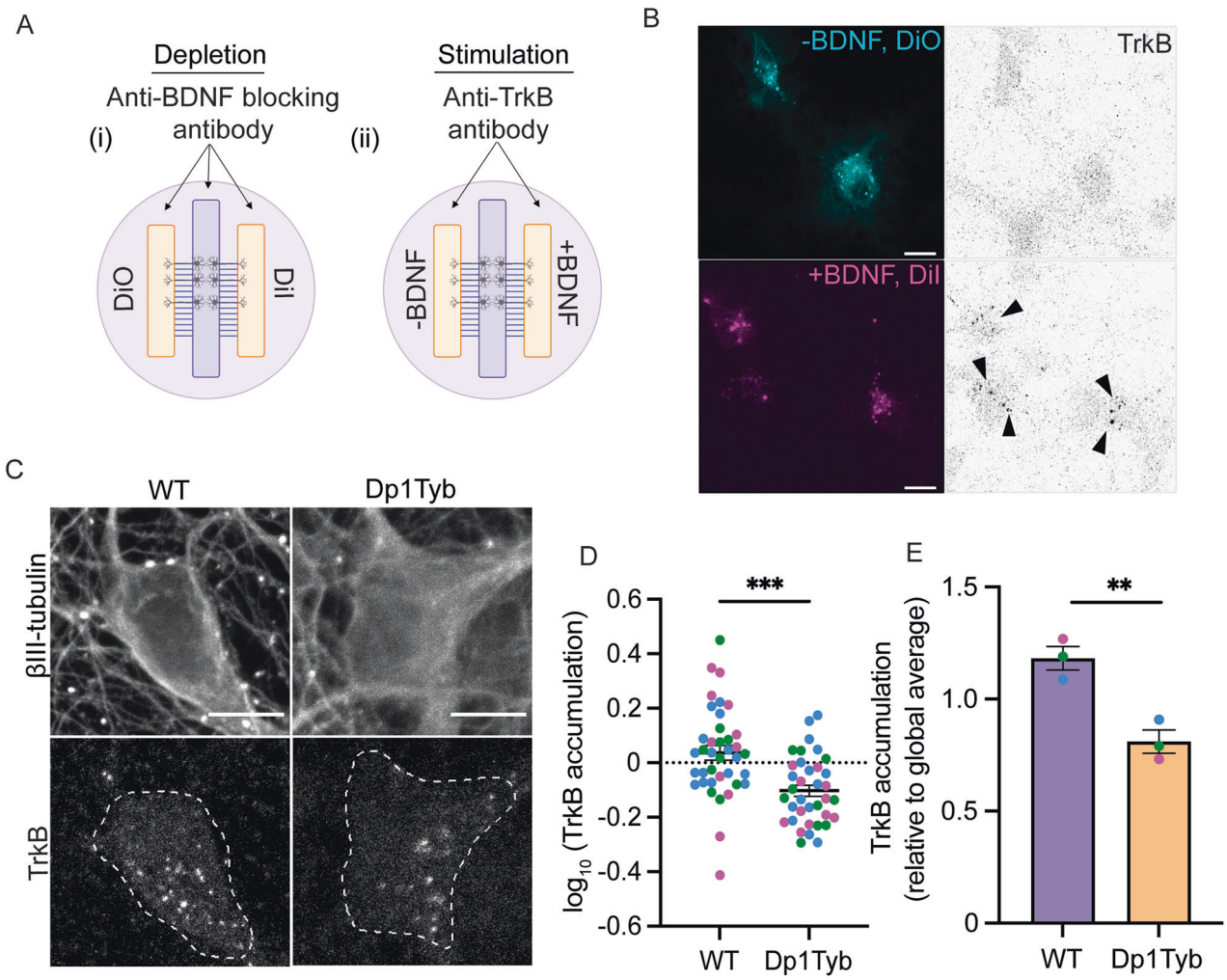



**Fig. 3 Reduced somatic accumulation of TrkB in Dp1Tyb basal forebrain neurons following axonal stimulation with BDNF. A** Schematic representation of the TrkB retrograde accumulation assay in three-chamber MFCs. **B** Representative confocal microscopy images of DiI and DiO retrograde tracers, and TrkB accumulation in the somatic compartment ± axonal BDNF treatment. **C** Representative images of TrkB accumulation in the soma following axonal incubation with anti-TrkB antibodies and BDNF in WT and Dp1Tyb neurons. **D**, **E** A significant decrease in the accumulation of TrkB in Dp1Tyb BFNs per cell (Student's *t* test; ***$p < 0.0001$) and per *N* (Student's *t* test; **$p = 0.0073$). Different coloured points represent individual *N*s. Bars represent mean ± SEM. $N = 3$ biological replicates. 10–15 cells per biological replicate. Scale bar = 10 µm.

signalling endosomes, alterations of these organelles due to deficits in sorting, transport and/or homoeostatic control, are likely to dampen trophic signalling and affect function both in vitro and in vivo [32, 43].

Previous BDNF/TrkB transport and signalling studies in AD-DS have been mainly conducted using the Ts65Dn mouse model, which is confounded by the presence of several additional duplicated mouse genes with an established endocytic function (e.g., *Snx9*, *Synj2*, *Dynlt1*, *Sylt3)* that are unrelated to Chr21 trisomy [49]. Furthermore, there is a lack of in vitro research investigating the relationship between trafficking and signalling of neurotrophin receptors in BFNs, one of the first populations of neurons to degenerate in AD and AD-DS [27, 57]. BFNs are reliant on target-derived trophic support for their survival, thus impaired neurotrophin receptor transport may explain their enhanced vulnerability to AD. Based on the known shortcomings of the Ts65Dn mouse model, we opted to investigate the post-endocytic trafficking of TrkB in BFNs derived from Dp1Tyb mice. This murine model includes triplication of only those genes on Mmu16 that are syntenic to Hsa21, including the mouse *App* gene. Furthermore, extensive physiological validation of many DS-related phenotypes has been recently provided in this mouse strain [47, 48, 58]. Here, by utilising primary BFNs grown in microfluidic devices, we uncovered endosomal abnormalities specifically in the axon, directly linking ERK signalling with impaired endosome transport.

Consistent with human post-mortem data in DS [35, 37], we observed a significant enlargement in early endosome size in Dp1Tyb BFNs compared to WT, making our approach relevant for studying endosome dynamics in AD-DS. Elevated Rab5 activity, as shown by increased levels of GTP-bound Rab5, has been suggested to underpin these morphological changes, leading to trafficking defects and neurodegeneration [50]. However, data concerning the hyperactivation of Rab5 are often derived from analyses performed in brain tissue, or whole cell lysates, rather than specifically in neurons. In this work, we identified increased levels of GTP-bound Rab5 in Dp1Tyb BFNs. Indeed, the level of active Rab5 significantly increased in WT neurons following 30 min of BDNF treatment, whereas it was elevated in Dp1Tyb neurons at steady state.

Recent evidence has shed light onto the pathway involving Rab5 hyperactivation and its downstream effects. Early to late endosome maturation is crucial for maintaining a functional endocytic pathway in neurons. A key step in this maturation process is the switch from Rab5 to Rab7, a transition that is

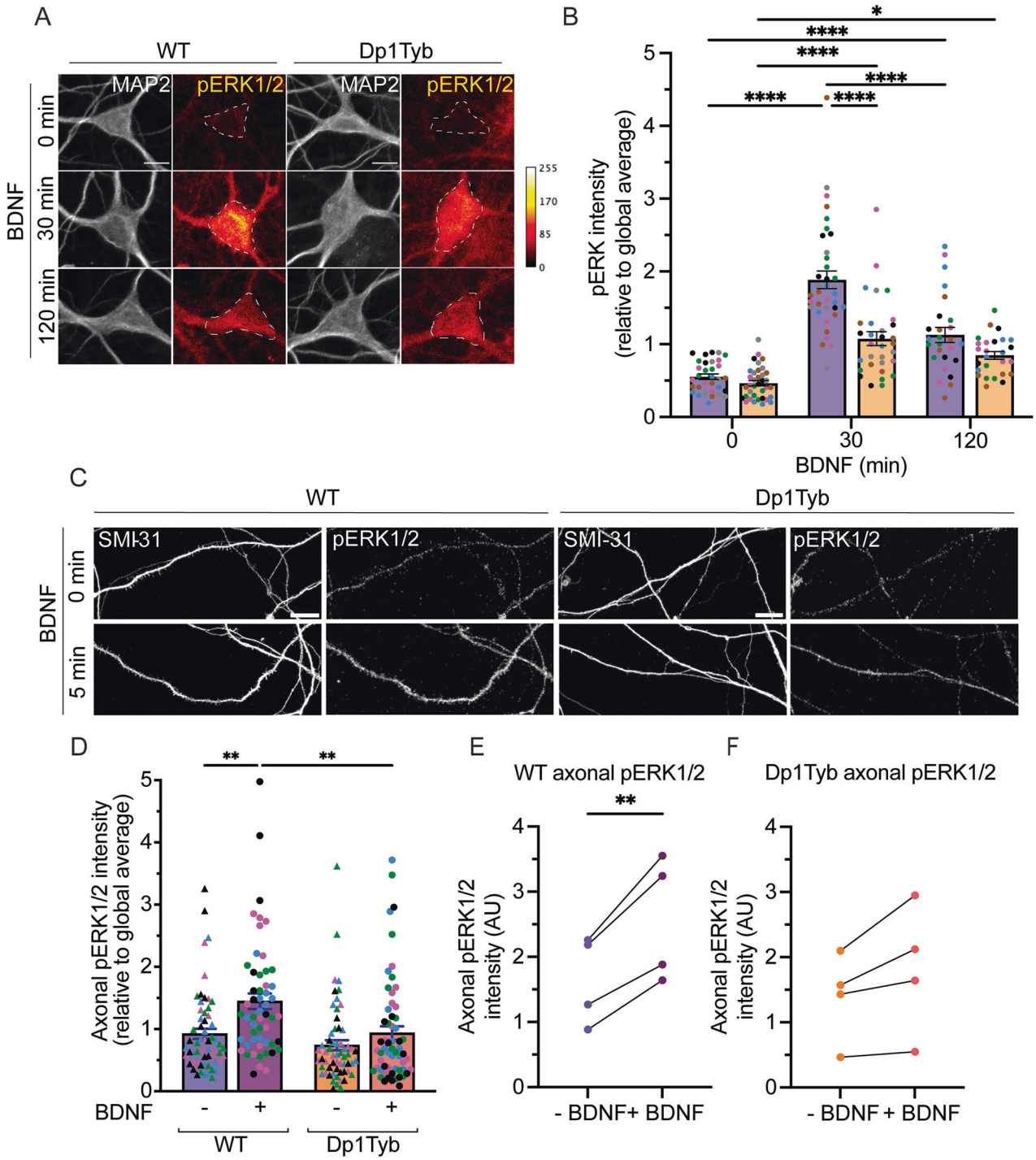



**Fig. 4 Selective impairment of ERK1/2 signalling following BDNF treatment in Dp1Tyb basal forebrain neurons. A** Representative confocal images of pERK1/2 staining in WT and Dp1Tyb neurons. **B** Quantification of pERK1/2 immunostaining. There was a significant effect of both BDNF treatment and genotype on ERK1/2 activation (2-way ANOVA with Tukey's multiple comparisons; BDNF treatment time; $^{****}p < 0.0001$, genotype; $^{****}p < 0.0001$ and interaction; $^{****}p < 0.0001$. Multiple comparisons; $^{****}p < 0.0001$, $^{*}p = 0.0195$). $N = 5$ biological replicates. Bars represent mean ± SEM. Coloured points represent individual *N*s. **C** Representative confocal images of pERK1/2 and SMI-31 staining in WT and Dp1Tyb axons ± BDNF treatment. **D** pERK1/2 intensity per axon in WT and Dp1Tyb BFNs ± 5 min BDNF treatment (2-way ANOVA with Tukey's multiple comparisons; BDNF treatment time; $^{***}p = 0.0004$; genotype; $^{***}p = 0.0006$. Multiple comparisons; $^{**}p = 0.0024$, $^{****}p < 0.0001$)). $N = 4$ biological replicates. Bars represent mean ± SEM. Coloured points represent individual *N*s. **E**, **F** BDNF treatment significantly increased the phosphorylation of ERK1/2 in WT BFN axons (paired Student's *t* test; $^{**}p = 0.0089$), but not in Dp1Tyb BFN axons (paired Student's *t* test; $p = 0.0915$). Scale bar = 10 µm.

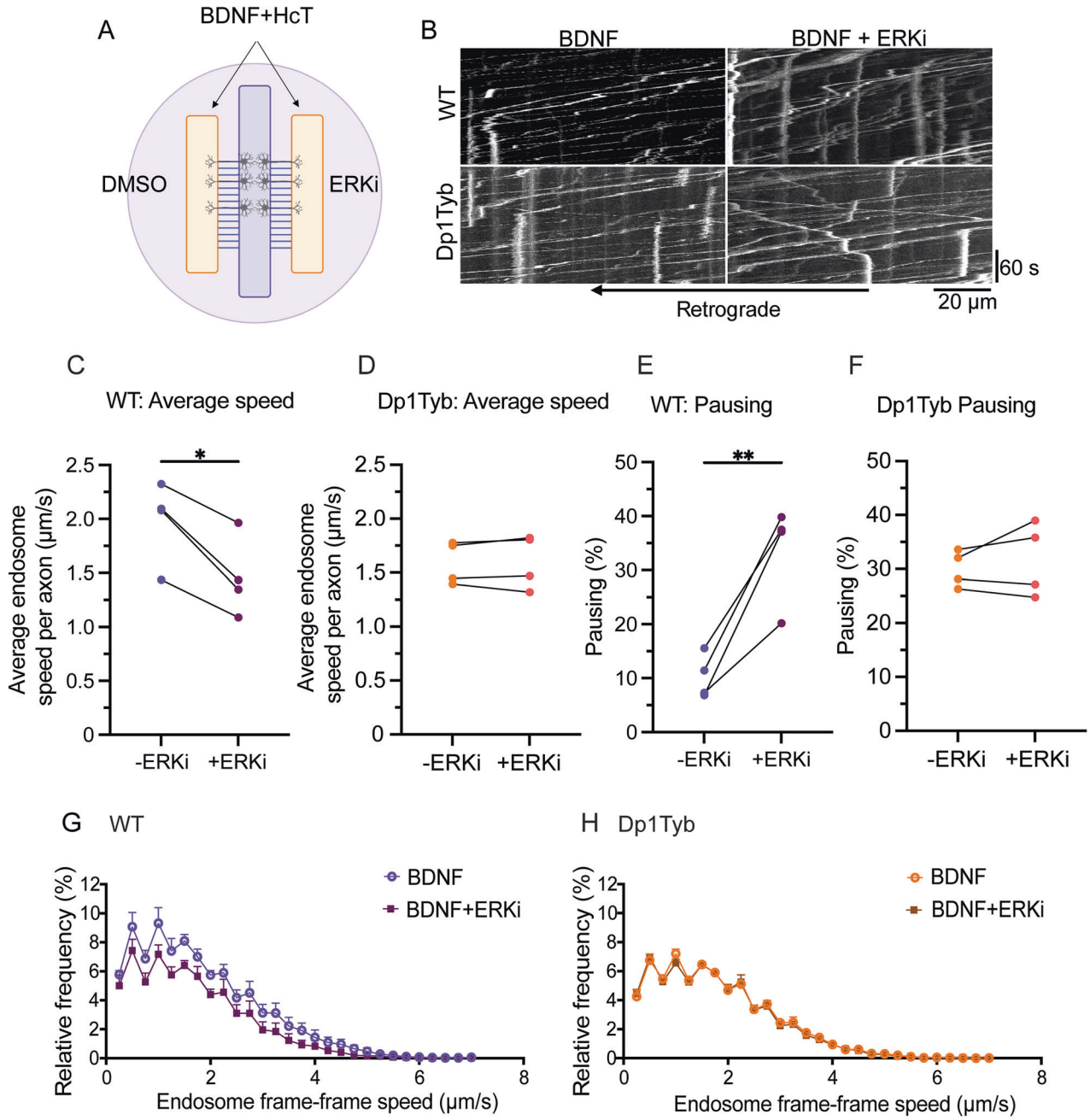



**Fig. 5 The axonal retrograde transport of signalling endosomes in Dp1Tyb basal forebrain neurons is not affected by ERK1/2 inhibition.** **A** Schematic depicting HcT-555 axonal transport experiment ± ERK inhibitor U0126. **B** Representative kymographs of HcT-555-positive signalling endosome transport in WT and Dp1Tyb BFNs ± U0126. **C**, **D** Average endosome speed per *N* in WT and Dp1Tyb BFNs in response to BDNF ± U0126. Lines represent paired conditions within the same three-chambers MFC. U0126 significantly reduces signalling endosome speed in WT (paired Student's *t* test; $*p = 0.0135$), but not in Dp1Tyb (paired Student's *t* test; $p = 0.7136$) BFNs. **E**, **F** Percentage of pausing of HcT-555-positive signalling endosomes in response to U0126 per *N*. Lines represent paired conditions within the same three-chamber MFC. U0126 significantly increases the percentage of pausing in WT (paired Student's *t* test; $**p = 0.0094$) but not Dp1Tyb (paired Student's *t* test; $p = 0.4571$) BFNs. **G**, **H** Endosome frame-frame speed distribution curve for signalling endosomes in WT and Dp1Tyb primary BFNs ± U0126 treatment. For all graphs $N = 4$ biological replicates, 5–8 axons imaged per condition. Endosome pausing (speed <0.25 µm/s) was excluded from the curves.

regulated by the Rab7-GEF complex MON1/CCZ1 and requires Rab5 inactivation [59, 60]. Hyperactivation of Rab5 may prevent this switch, blocking progression of receptors and other cargo through the endolysosomal pathway, leading to cellular dysfunction. In DS, hyperactivation of Rab5 due to increased *APP* gene dosage disrupts this equilibrium, leading to failed maturation of endosomal compartments downstream of early endosomes [44]. Furthermore, overactivation of Rab5 alone is sufficient to cause synaptic dysfunction, tau hyperphosphorylation and neurodegeneration both in vitro and in vivo demonstrating a causal role for Rab5 overactivation in AD-related pathways [50]. Conversely, targeted reduction of Rab5 using antisense oligonucleotides in the Dp16 mouse model of DS restores endosomal structure and ameliorates deficits in BDNF-TrkB signalling, tau phosphorylation and synaptic density [61].

Functional Rab5 is required for the long-distance propagation of the BDNF signal [13]. Accordingly, we identified selective deficits in the axonal retrograde transport of BDNF-TrkB signalling endosomes in Dp1Tyb BFNs. Whereas BDNF significantly enhanced signalling endosome speeds and reduced pausing in WT BFNs, as observed in other types of neurons [56, 62–64], these effects were blunted in Dp1Tyb neurons. Rab5 has been associated with endosomes that undergo less processive axonal transport [13, 65]. Therefore, if receptors are being retained in enlarged Rab5-positive endosomes, thus preventing their transition to Rab7 organelles, slower velocities and increased pausing might be expected, as we found in Dp1Tyb BFNs. Furthermore, our retrograde accumulation assay demonstrated reduced TrkB transport to the soma, confirming a specific impairment in long-range BDNF-TrkB trafficking in Dp1Tyb BFNs. These findings align with reports of disrupted neurotrophic signalling in models of AD-DS [32, 34, 43]. Future studies are required to determine mechanistically how Rab5 hyperactivation impacts the maturation and function of Rab7-positive endosomes in this specific model.

BDNF-activated TrkB orchestrates its own trafficking through recruitment of effector proteins to early endosomes [66]. This recruitment is essential for the maturation and motility of signalling endosomes. In hippocampal neurons, BDNF-activated TrkB traffics through APPL1-positive endosomes to signalling endosomes, a process which requires effectors endophilin A1 and retrolinkin [66]. Interestingly, an abnormally high recruitment of APPL1 to Rab5-positive compartments has been found in DS fibroblasts displaying enlarged early endosomes and Rab5 hyperactivation [45]. Conversely, APPL1 depletion using siRNA reversed both endosomal enlargement and transport defects in neurons overexpressing APP and Rab5 [45]. The failure of BDNF to induce normal endosome motility in Dp1Tyb BFNs may reflect an inability of Rab5-positive compartments to transition into competent signalling endosomes or to engage the transport machinery required for long-range movement of cargoes.

BDNF signalling drives the phosphorylation of several microtubule associated proteins (MAPs) in human iPSC-derived lower motor neurons [64], and ERKs have been shown to regulate the microtubule landscape [67]. Our data revealed reduced ERK1/2 activation in Dp1Tyb BFNs in response to BDNF, not only in the somatodendritic compartment, but also in axons. Since ERK1/2 activation is critical for BDNF-mediated endosomal dynamics [55, 56] we hypothesised that inhibiting ERK1/2 might phenocopy the defects observed in the Dp1Tyb BFNs. Consistent with this hypothesis, pharmacological inhibition of ERK1/2 reduced transport speeds and increased pausing in WT BFNs treated with BDNF, mirroring the transport deficits seen in Dp1Tyb BFNs. These findings suggest a mutual regulation between trafficking and signalling, wherein defects in sorting from early endosomes impair ERK1/2 activation, which further disrupts axonal transport. Indeed, disrupting early endosome trafficking through depletion of retrolinkin or endophilin A1 also impaired acute ERK activation in hippocampal neurons [66]. This dynamic interplay highlights a bidirectional relationship between endosomal signalling and trafficking, potentially amplifying pathological effects. Elucidating the exact point of disruption in this feedback mechanism, and how this relates to the abnormal endosome morphology in Dp1Tyb BFNs warrant future studies.

ERK1/2 activation has been shown to enable the recruitment of the dynein intermediate chain to signalling endosomes in neurons [55]. Furthermore, expression of an intermediate chain that could not be phosphorylated by ERK1/2 and recruit TrkB resulted in a 45% decrease in cell survival, highlighting the importance of ERK1/2-dependent signalling for long-distance neurotrophin functions [55]. Crucially, we found that ERK1/2 inhibition had no effect on axonal transport in Dp1Tyb neurons. The lack of effect is consistent with a basal impairment of ERK1/2 signalling in Dp1Tyb neurons occurring downstream of early endosome abnormalities. These upstream defects likely limit the capacity of BDNF to elicit a physiological signalling response in these neurons, making the pharmacological inhibition of ERK1/2 inconsequential to the already compromised transport and signalling dynamics.

Retrograde transport relies on cytoplasmic dynein forming a complex with its cofactor, dynactin, and specific dynein adaptors [68]. ERK1/2 activation might result in an increased local translation of dynein cofactors and/or adaptor proteins. Indeed, mRNAs encoding dynein regulators have been found in the axon in the central and peripheral nervous systems [69–71]. In dorsal root ganglia (DRG) neurons, axonal transcripts of the dynein adaptor protein LIS1, and the dynactin subunit p150$^{Glued}$ are translated in response to increased NGF signalling. Inhibition of protein synthesis using anisomycin, or knockdown of mRNA transcripts for *LIS1* or *p150*$^{Glued}$, abolished the NGF-induced increase in the retrograde transport of lysosomes and quantum dot-conjugated NGF [71]. Interestingly, only NGF-induced, rather than basal, axonal transport seems dependent on local translation, possibly reflecting previously inactive dynein complexes becoming activated and bound to cargo in response to NGF. This result might be relevant to the present study given that the transport deficits in Dp1Tyb BFNs are only evident upon BDNF stimulation, suggesting that neurotrophin signalling endosomes are specifically impaired.

Similar mechanisms have been identified in primary motor neurons, with IGFR1 inhibition leading to increased local translation of the dynein adaptor BICD2 and the subsequent enhancement of signalling endosome transport [53, 62]. The impaired BDNF response in Dp1Tyb BFNs may therefore reflect defects in axonal translation of dynein associated proteins or altered MAP phosphorylation due to altered ERK1/2 activation.

The dysregulation of early endosome morphology and function, coupled with impaired BDNF transport and signalling, might highlight a potential convergence of pathogenic mechanisms in AD-DS. A limitation of our study is that we utilised mixed BFN cultures comprising both cholinergic and non-cholinergic populations, all of which express TrkB. While this approach captures broader endosomal trafficking defects, it may not fully reflect the specific vulnerabilities and signalling dynamics of cholinergic neurons. Future studies isolating or enriching for cholinergic neurons will be essential to determine whether these mechanisms are uniquely modulated within this neuronal subtype. Our results emphasise the need for targeted therapeutic strategies that address endosomal trafficking defects and signalling impairments. Future studies should investigate the precise molecular mechanisms linking increased levels of GTP-Rab5 and dampened ERK1/2 signalling to TrkB transport deficits in AD-DS models.

## MATERIALS AND METHODS

### Animals

C57BL/6 J;129P2-Dp(16*Lipi-Zbtb21*)1TybEmcf mice (hereafter referred to as Dp1Tyb) were maintained on a C57BL/6 J background for more than ten generations [47, 48]. Animals were housed in a temperature and humidity-controlled environment with a 12 h light/dark cycle, with access to food and water ad libitum. Timed matings were set with Dp1Tyb males and C57BL/6 J females. Embryos were collected 16 days after the detection of a positive plug (E16) and genotype confirmed by PCR using the following primer pairs (Forward: CTAACCCTAACCCTAAGTCCTTGTC, Reverse: TGAGGAGAGTTTTCTGGGAGAA; Forward: CGGGCCTCTTCGCTATTACG, Reverse: GAGTGCATTCTCCTCATTCAGATG) and PCR cycling conditions (initial denaturation at 94 °C for 3 min; 35 cycles of denaturation at 94 °C for 30 s, annealing at 57 °C for 10 s, and elongation at 72 °C for 1 min; followed by a final extension at 72 °C for 7 min).

All experiments were conducted under the guidelines of the UCL Genetic Manipulation and Ethics Committees and in accordance with the European Community Council Directive of 22 September 2010 (2010/63/EU). All procedures for the care and treatment of animals were carried out under license from the U.K. Home Office in accordance with the Animals (Scientific Procedures) Act 1986 Amendment Regulations 2012.

### Plasmids and reagents

Reagents were from Sigma-Aldrich unless otherwise stated. Recombinant human NGF and BDNF were purchased from PeproTech. pGEX-4T-2/Rabaptin-5:R5BD was a gift from Guangpu Li (Addgene plasmid # 168808; http://n2t.net/addgene:168808; RRID:Addgene_168808) [72]. ERK inhibitor U1026 was from Promega (V1121). Primary antibodies for immunofluorescence (IF) and western blot (WB) were sourced as follows: MAP2 (Abcam, ab5392, RRID:AB_2138153, IF 1:2,000), SMI-31 (BioLegend, 801601, RRID:AB_2564641, IF 1:300), ERK1/2 (4695, RRID:AB_390779, IF 1:250, WB 1:1,000), pERK1/2$_{Thr202/Tyr204}$ (9101, RRID:AB_331646, IF 1:250, WB 1:1,000), AKT (9272S, RRID:AB_329827, IF 1:250, WB 1:1,00), pAKT(Ser473) (Cell Signalling Technology 4060S, RRID:AB_2315049, IF 1:250, WB 1:1,000), TrkB (R&D Systems, AF1494, RRID:AB_2155264, IF 1:250, WB 1:500), EEA1 (BD Transduction Laboratories, 610457, RRID:AB_397830, IF 1:500), GST (Abcam, ab9085, RRID:AB_306993, IF 1:500), and GADPH (Sigma Aldrich, MAB374, RRID:AB_2107445, WB 1:1,000). Antibodies used for the TrkB internalisation assays were as follows: TrkB (Merck (Millipore) AB9872, RRID:AB_2236301, 1:50) and BDNF (BioTechne, AF248, RRID:AB_355275, 1:50).

### BFN culture

The basal forebrain (BF) from Dp1Tyb and WT embryos of either sex was dissected at E16 in Hank's balanced salt solution (HBSS) and transferred in Hibernate E medium (ThermoFisher, #A1247601). Tissue was washed in HBSS prior to incubating in Accumax (Innovative Cell Technologies, #AM105) for 10 min, then diluted (1:1) in HBSS for a further 5 min. Tissue was resuspended in warm plating medium (Minimum Essential Medium (MEM; Gibco) supplemented with 10% heat inactivated horse serum, 38 mM NaCl, 0.6% glucose and 1 × GlutaMAX (Invitrogen) prior to mechanical dissociation by pipetting. 10–15,000 cells per $cm^2$ were seeded onto glass coverslips or microfluidic chambers (MFCs) pre-coated with 1 mg/mL poly-L-lysine. Fabrication and coating of MFCs was conducted as described previously [62]. Two hours after plating, medium was changed to maintenance medium (Neurobasal; Gibco) supplemented with 1% penicillin/streptomycin (ThermoFisher), 38 mM NaCl, 0.6% glucose, 1× GlutaMAX, 1× B27 (Gibco), 10 ng/mL NGF and 10 ng/mL BDNF). Cultures were maintained in a humidified incubator at 37 °C, 5% $CO_2$. Medium was half changed every 3–5 days. After 3 days in vitro (DIV) the axonal compartment of each MFC was supplemented with 20 ng/mL BDNF and NGF to encourage axonal growth; the somatic compartment was maintained with 10 ng/mL BDNF and NGF.

### Recombinant proteins

The Rabaptin-5(R5BD) fusion protein was produced in chemically competent NEB 5-alpha *E. coli* (New England Biolabs) transformed with the pGEX-4T-2/Rabaptin-5:R5BD plasmid. Protein expression was induced by treatment with 0.5 mM isopropyl β-D-1-thiogalactopyranoside (IPTG) for 4 h. Cells were harvested by centrifugation at 4000 × *g* for 30 min at 4 °C. The pellet was resuspended in 50 mM Tris HCl (pH 7.5), 150 mM NaCl, 0.05% Tween-20, 2 mM EDTA, 0.1% 2-mercaptoethanol (βME) and Halt protease and phosphatase inhibitor cocktail (1:100, ThermoFisher). Bacteria were lysed by sonication with 4 ×15 s pulses at 40 kHz. The bacterial lysate was centrifuged at 10,000 × *g* for 40 min and the pellet discarded. Rabaptin-5(R5BD) was purified using glutathione-agarose beads (Merck-Millipore) as per manufacturer's instructions and eluted using 10 mM reduced glutathione (pH 8.0). Purified proteins were dialysed using Slide-A-Lyzer G2 Dialysis Cassettes (ThermoFisher, #87735) to remove the reduced glutathione and Ultra-0.5 mL centrifugal filters with a 10 kDa cut off (Amicon) were used to concentrate proteins post dialysis.

### Rab5 activity assay

Rab5 activity was determined using a protocol adapted from Moya-Alvarado et al [17]. Neurons cultured on coverslips were depleted of endogenous growth factors for 2 h prior to stimulation with 50 ng/mL BDNF for 0, 5 or 30 min. Cells were washed in PBS and briefly fixed for 8 min with 4% PFA, 4% sucrose in PBS before blocking for 45 min in 3% BSA reconstituted in incubation buffer (50 mM Tris-Cl, 50 mM NaCl, 5 mM $MgCl_2$, 1 mM EDTA, 0.25 mM sucrose, 0.2% Triton X-100 and 0.5 mM dithiothreitol (DTT) added fresh; pH 7.2). GST-Rabaptin5R5BD and GST were purified and diluted to 15 µg/mL in incubation buffer. 10 µM reduced glutathione was added to the buffer to reduce formation of aggregates. Diluted proteins were centrifuged at 20,000 × g for 30 min prior to applying to the neurons overnight at 4 °C with shaking. The following day cells were washed briefly 5 times with PBS and refixed for 15 min with 4% PFA, 4% sucrose for anti-GST immunofluorescence.

### Surface TrkB staining assay

BFNs were kept in Neurobasal for 1 h and prior to incubating on ice with 1:50 anti-TrkB rabbit antibody (Millipore AB9872). Neurons were quickly rinsed twice in cold-PBS, fixed in 3% PFA, 4% sucrose in PBS and processed for immunofluorescence. Surface TrkB was labelled with donkey anti-rabbit AlexaFluor647 secondary antibody under non-permeabilizing conditions. To identify the axon, neurons were incubated with SMI-31 (Biolegend 837904) 1:500 in 3% BSA, 0.05% saponin for 1 h. Following three washes with cold PBS, the neurons were incubated with a donkey anti-mouse AlexaFluor488 secondary antibody (1:500) for 1 h.

### Immunoendocytosis

To confirm the presence of TrkB in $H_cT$ carriers, BFNs were starved in Neurobasal for 1 h prior to incubating on ice with 1:50 anti-TrkB rabbit antibody (Millipore AB9872) and 30 nM AlexaFluor555-$H_cT$ in ice cold Neurobasal for 1 h. Following two washes with warm Neurobasal, BFNs were incubated with 50 ng/ml BDNF for 1 h at 37 °C to induce internalisation of TrkB. The neurons were rinsed three times with cold PBS and the remaining surface-bound anti-TrkB antibody and AlexaFluor555-$H_cT$ were dissociated by washing twice with an acid solution (0.2 M acetic acid, 0.5 M NaCl, pH 3.2). Neurons were rinsed with PBS and then fixed with 3% PFA 4% sucrose in PBS. Neurons were permeabilised and incubated with an SMI-31 antibody and further incubated with and anti-mouse AlexaFluor488-conjugated antibody (1:500), anti-rabbit Alexa Fluor647-conjugated antibody (1:500); nuclei were counterstained with DAPI 1:4,000.

### Axonal retrograde transport

At DIV 14, neurons grown in three-chamber MFCs were depleted of endogenous growth factors for 2 h in Neurobasal. For the final 30 min of depletion, axonal compartments were supplemented with 30 nM AlexaFluor555-$H_cT$ [53, 62]. Axons were incubated in the presence or absence of 50 ng/mL BDNF for 30 min. All media was then replaced with Neurobasal supplemented with 20 nM HEPES-NaOH (pH 7.4) and imaged (Zeiss LSM 980 with Airyscan 2). In the BDNF conditions, the Neurobasal/HEPES-NaOH was supplemented with 50 ng/mL BDNF in the axonal compartment for imaging. During image acquisition, neurons were kept at 37 °C in the humidified chamber of the microscope. Each MFC was imaged for approximately 40 min, acquiring videos at 2 frames/s from 5 to 8 axons per condition. For ERK1/2 inhibitor experiments, axonal compartments were incubated with 50 ng/mL BDNF, 30 nM $H_cT$ in the presence of 20 µM U0126 or an equivalent amount of DMSO.

### Somatic accumulation of TrkB

The retrograde accumulation of TrkB was assessed using an established protocol with minor modifications [19]. Neurons were grown in three-chamber MFCs. 24 h before the experiment, axonal compartments were incubated with 10 ng/mL of the lipophilic retrograde tracers DiI (Invitrogen, D3911) and DiO (Invitrogen, D275). Having two different retrograde tracers enables identification of neurons projecting axons to each compartment. On DIV14, the media was replaced with Neurobasal and an anti-BDNF blocking antibody (1:50, BioTechne, AF248). After 2 h, axonal compartments were washed with Neurobasal and axons incubated with polyclonal antibodies against the extracellular domain of TrkB (Merck Millipore, AB9872) together with 50 ng/mL BDNF or an anti-BDNF blocking antibody (1:50). After 2.5 h, neurons were fixed with 4% PFA, 4% sucrose in PBS. To reveal the somatic accumulation of TrkB antibodies, cells were blocked and permeabilised in 4% BSA, 0.2% saponin for 1 h followed by incubation with Alexa Fluor-conjugated secondary antibodies.

### Signalling assays

Neurons cultured on coverslips, in 6-well plates, or MFCs were depleted of endogenous growth factors by incubation in Neurobasal for 2 h before stimulation with 50 ng/mL BDNF for 0, 5, 30 or 120 min to establish a time course of ERK1/2 and AKT activation in BFNs. Cells on coverslips and MFCs were fixed with 4% PFA, 4% sucrose, and the phosphorylation of ERK1/2 and AKT in the soma and/or axons was analysed by IF and confocal microscopy. Following the BDNF time course in 6-well plates, cells were lysed on ice in RIPA buffer (50 mM Tris-HCl pH 7.5, 150 mM NaCl, 1% NP-40, 0.5% sodium deoxycholate, 0.1% sodium dodecyl sulphate, 1 mM EDTA, 1 mM EGTA) with Halt protease and phosphatase inhibitor cocktail (1:100, ThermoFisher), and the phosphorylation of ERK1/2 and AKT was analysed by western blotting.

### Immunofluorescence

Neurons were washed in PBS and fixed for 15 min in 4% PFA, 4% sucrose prior to incubation in 0.15 M glycine (pH 7.0) in PBS for 10 min. Neurons were blocked and permeabilised in 4% BSA, 0.2% saponin in PBS for 1 h before incubating with primary antibodies diluted in 4% BSA, 0.05% saponin in PBS overnight at 4 °C. Samples were washed three times with PBS and incubated for 1 h with AlexaFluor-conjugated secondary antibodies and 4′,6-diamidino-2-phenylindole (DAPI) (1:500) diluted in 4% BSA, 0.05% saponin in PBS. Finally, neurons were washed in PBS and mounted using Fluoromount-G (Invitrogen).

### Western blotting

Purified proteins or cell lysates were mixed with 4× Laemmli buffer (250 mM Tris-HCl, pH 6.8 8% SDS, 40% glycerol, 0.02% bromophenol blue) and 10% fresh βME and denatured at 100 °C for 5 min. BCA protein Assay Kit (ThermoFisher) was used to quantify the protein concentration. Proteins were separated using 4–15% Mini-PROTEAN TGX Stain-Free Protein Gels (Bio-Rad) and transferred onto methanol-activated polyvinylidene difluoride (PVDF) membranes with the semi dry Trans-Blot Turbo Transfer system (Bio-Rad). Membranes were blocked in 5% BSA in PBS with 0.1% Tween 20 (PBS-T) for 1 h at room temperature. Primary antibodies were incubated overnight at 4 °C with shaking. Membranes were washed three times with PBS-T for 10 min before incubation with the appropriate horseradish peroxidase (HRP) conjugated secondary antibody (DAKO) for 1 h at room temperature. After three 10 min washes with PBS-T, Immobilon Crescendo Western HRP Substrate (Merck-Millipore) was used for chemiluminescent detection of proteins using the ChemiDoc Touch Imaging System.

### Image acquisition and quantification

All images were acquired using the Zeiss LSM 980 confocal microscope with Airyscan 2 using an oil immersion 40×/1.3 numerical aperture (NA) or 63×/1.4 NA objectives unless otherwise stated. Fixed samples were imaged as Z-stacks. For time-lapse imaging of live neurons, images were acquired at 2 frames/s. Images were analysed using Image J/FIJI (version 2.1.0, 1.53c) [73]. For the analysis of signalling endosome dynamics, the FIJI plugin Trackmate [74] was used to manually track all retrogradely moving organelles. Endosomes were selected and manually connected in each adjacent frame giving single frame-frame velocities which were then averaged across the entire track, giving an average speed for each endosome. The endosome speed was then averaged per axon and per biological replicate (N). A biological replicate is defined as mouse embryos of the same genotype pooled from one litter. Speed distribution curves were generated to display the relative frame-frame movement of all signalling endosomes. A pause was defined as a signalling endosome that moved with a speed less than 0.25 µm/s between consecutive frames. The percentage of time paused was determined by the number of pauses divided by the total number of frame-frame movements per axon. This was then averaged per *N*.

Western blot bands were quantified using Image Lab (Bio-Rad, version 6.1.0).

### Statistical analysis

Data was analysed and visualised using GraphPad Prism 9 (La Jolla, California, USA, version 9.4.1) and tested for normality and homoscedasticity. Where assumptions were not met, data was log transformed. For analyses with >2 groups, a two-way ANOVA was used to compare means followed by Tukey's multiple comparisons. For comparison of two groups, Student's *t* test was used. Levels of significance are indicated in figure legends. Welch's test was conducted where equal variance was not assumed. Mean ± standard error is shown. Sample size was determined based on previous experiments from the laboratory. The investigator was blinded to experimental group during data analysis.

## DATA AVAILABILITY

All data are provided in the main text.

## REFERENCES

1. Chao MV. Neurotrophins and their receptors: a convergence point for many signalling pathways. Nat Rev Neurosci. 2003;4:299–309.
2. Meeker RB, Williams KS. The p75 neurotrophin receptor: at the crossroad of neural repair and death. Neural Regen Res. 2015;10:721–5.
3. Szobota S, Mathur PD, Siegel S, Black K, Saragovi HU, Foster AC. BDNF, NT-3 and Trk receptor agonist monoclonal antibodies promote neuron survival, neurite extension, and synapse restoration in rat cochlea ex vivo models relevant for hidden hearing loss. PLoS ONE. 2019;14:e0224022.
4. Woo D, Seo Y, Jung H, Kim S, Kim N, Park SM, et al. Locally activating TrkB receptor generates actin waves and specifies axonal fate. Cell Chem Biol. 2019;26:1652–63 e4.
5. Villarroel-Campos D, Schiavo G, Lazo OM. The many disguises of the signalling endosome. FEBS Lett. 2018;592:3615–32.
6. Segal RA, Greenberg ME. Intracellular signaling pathways activated by neurotrophic factors. Annu Rev Neurosci. 1996;19:463–89.
7. Moya-Alvarado G, Tiburcio-Felix R, Ibanez MR, Aguirre-Soto AA, Guerra MV, Wu C, et al. BDNF/TrkB signaling endosomes in axons coordinate CREB/mTOR activation and protein synthesis in the cell body to induce dendritic growth in cortical neurons. Elife. 2023;12:e77455.
8. Moya-Alvarado G, Valero-Pena X, Aguirre-Soto A, Bustos FJ, Lazo OM, Bronfman FC. PLC-gamma-Ca(2+) pathway regulates axonal TrkB endocytosis and is required for long-distance propagation of BDNF signaling. Front Mol Neurosci. 2024;17:1009404.
9. Olenick MA, Dominguez R, Holzbaur ELF. Dynein activator Hook1 is required for trafficking of BDNF-signaling endosomes in neurons. J Cell Biol. 2019;218:220–33.
10. Zhou B, Cai Q, Xie Y, Sheng ZH. Snapin recruits dynein to BDNF-TrkB signaling endosomes for retrograde axonal transport and is essential for dendrite growth of cortical neurons. Cell Rep. 2012;2:42–51.
11. Wu C, Ramirez A, Cui B, Ding J, Delcroix JD, Valletta JS, et al. A functional dynein-microtubule network is required for NGF signaling through the Rap1/MAPK pathway. Traffic. 2007;8:1503–20.
12. Homma Y, Hiragi S, Fukuda M. Rab family of small GTPases: an updated view on their regulation and functions. FEBS J. 2021;288:36–55.
13. Deinhardt K, Salinas S, Verastegui C, Watson R, Worth D, Hanrahan S, et al. Rab5 and Rab7 control endocytic sorting along the axonal retrograde transport pathway. Neuron. 2006;52:293–305.
14. Harrington AW, Ginty DD. Long-distance retrograde neurotrophic factor signalling in neurons. Nat Rev Neurosci. 2013;14:177–87.
15. Wu C, Cui B, He L, Chen L, Mobley WC. The coming of age of axonal neurotrophin signaling endosomes. J Proteom. 2009;72:46–55.
16. Lazo OM, Gonzalez A, Ascano M, Kuruvilla R, Couve A, Bronfman FC. BDNF regulates Rab11-mediated recycling endosome dynamics to induce dendritic branching. J Neurosci. 2013;33:6112–22.
17. Moya-Alvarado G, Gonzalez A, Stuardo N, Bronfman FC. Brain-Derived Neurotrophic Factor (BDNF) regulates Rab5-positive early endosomes in hippocampal neurons to induce dendritic branching. Front Cell Neurosci. 2018;12:493.
18. Gonzalez-Gutierrez A, Lazo OM, Bronfman FC. The Rab5-Rab11 endosomal pathway is required for BDNF-induced CREB transcriptional regulation in hippocampal neurons. J Neurosci. 2020;40:8042–54.
19. Lazo OM, Schiavo G. Rab10 regulates the sorting of internalised TrkB for retrograde axonal transport. Elife. 2023;12:e81532.
20. Sleigh JN, Rossor AM, Fellows AD, Tosolini AP, Schiavo G. Axonal transport and neurological disease. Nat Rev Neurol. 2019;15:691–703.
21. Berth SH, Lloyd TE. Disruption of axonal transport in neurodegeneration. J Clin Invest. 2023;133:3–8.
22. Cai Y, Zhang XM, Macklin LN, Cai H, Luo XG, Oddo S, et al. BACE1 elevation is involved in amyloid plaque development in the triple transgenic model of Alzheimer's disease: differential Abeta antibody labeling of early-onset axon terminal pathology. Neurotox Res. 2012;21:160–74.
23. Gilley J, Seereeram A, Ando K, Mosely S, Andrews S, Kerschensteiner M, et al. Age-dependent axonal transport and locomotor changes and tau hypophosphorylation in a "P301L" tau knockin mouse. Neurobiol Aging. 2012;33:621.e1–15.
24. Stokin GB, Lillo C, Falzone TL, Brusch RG, Rockenstein E, Mount SL, et al. Axonopathy and transport deficits early in the pathogenesis of Alzheimer's disease. Science. 2005;307:1282–8.
25. Fortea J, Zaman SH, Hartley S, Rafii MS, Head E, Carmona-Iragui M. Alzheimer's disease associated with Down syndrome: a genetic form of dementia. Lancet Neurol. 2021;20:930–42.
26. Wiseman FK, Al-Janabi T, Hardy J, Karmiloff-Smith A, Nizetic D, Tybulewicz VL, et al. A genetic cause of Alzheimer disease: mechanistic insights from Down syndrome. Nat Rev Neurosci. 2015;16:564–74.
27. Martinez JL, Zammit MD, West NR, Christian BT, Bhattacharyya A. Basal forebrain cholinergic neurons: linking down syndrome and Alzheimer's disease. Front Aging Neurosci. 2021;13:703876.
28. Mufson EJ, Perez SE. The cholinotrophic system in Down syndrome. Handb Clin Neurol. 2025;211:185–213.
29. Granholm AC, Sanders LA, Crnic LS. Loss of cholinergic phenotype in basal forebrain coincides with cognitive decline in a mouse model of Down's syndrome. Exp Neurol. 2000;161:647–63.

30. Peng S, Wuu J, Mufson EJ, Fahnestock M. Precursor form of brain-derived neurotrophic factor and mature brain-derived neurotrophic factor are decreased in the pre-clinical stages of Alzheimer's disease. J Neurochem. 2005;93:1412–21.
31. Cooper JD, Salehi A, Delcroix JD, Howe CL, Belichenko PV, Chua-Couzens J, et al. Failed retrograde transport of NGF in a mouse model of Down's syndrome: reversal of cholinergic neurodegenerative phenotypes following NGF infusion. Proc Natl Acad Sci USA. 2001;98:10439–44.
32. Salehi A, Delcroix JD, Belichenko PV, Zhan K, Wu C, Valletta JS, et al. Increased App expression in a mouse model of Down's syndrome disrupts NGF transport and causes cholinergic neuron degeneration. Neuron. 2006;51:29–42.
33. Nosheny RL, Belichenko PV, Busse BL, Weissmiller AM, Dang V, Das D, et al. Increased cortical synaptic activation of TrkB and downstream signaling markers in a mouse model of Down Syndrome. Neurobiol Dis. 2015;77:173–90.
34. Chen XQ, Salehi A, Pearn ML, Overk C, Nguyen PD, Kleschevnikov AM, et al. Targeting increased levels of APP in Down syndrome: Posiphen-mediated reductions in APP and its products reverse endosomal phenotypes in the Ts65Dn mouse model. Alzheimers Dement. 2021;17:271–92.
35. Cataldo AM, Petanceska S, Terio NB, Peterhoff CM, Durham R, Mercken M, et al. Abeta localization in abnormal endosomes: association with earliest Abeta elevations in AD and Down syndrome. Neurobiol Aging. 2004;25:1263–72.
36. Cataldo AM, Rebeck GW, Ghetri B, Hulette C, Lippa C, Van Broeckhoven C, et al. Endocytic disturbances distinguish among subtypes of Alzheimer's disease and related disorders. Ann Neurol. 2001;50:661–5.
37. Cataldo AM, Peterhoff CM, Troncoso JC, Gomez-Isla T, Hyman BT, Nixon RA. Endocytic pathway abnormalities precede amyloid beta deposition in sporadic Alzheimer's disease and Down syndrome: differential effects of APOE genotype and presenilin mutations. Am J Pathol. 2000;157:277–86.
38. Cataldo AM, Petanceska S, Peterhoff CM, Terio NB, Epstein CJ, Villar A, et al. App gene dosage modulates endosomal abnormalities of Alzheimer's disease in a segmental trisomy 16 mouse model of down syndrome. J Neurosci. 2003;23:6788–92.
39. Choi JH, Kaur G, Mazzella MJ, Morales-Corraliza J, Levy E, Mathews PM. Early endosomal abnormalities and cholinergic neuron degeneration in amyloid-beta protein precursor transgenic mice. J Alzheimers Dis. 2013;34:691–700.
40. Spencer B, Desplats PA, Overk CR, Valera-Martin E, Rissman RA, Wu C, et al. Reducing Endogenous alpha-Synuclein mitigates the degeneration of selective neuronal populations in an alzheimer's disease transgenic mouse model. J Neurosci. 2016;36:7971–84.
41. Sawa M, Overk C, Becker A, Derse D, Albay R, Weldy K, et al. Impact of increased APP gene dose in Down syndrome and the Dp16 mouse model. Alzheimers Dement. 2022;18:1203–34.
42. Jiang Y, Rigoglioso A, Peterhoff CM, Pawlik M, Sato Y, Bleiwas C, et al. Partial BACE1 reduction in a Down syndrome mouse model blocks Alzheimer-related endosomal anomalies and cholinergic neurodegeneration: role of APP-CTF. Neurobiol Aging. 2016;39:90–8.
43. Xu W, Weissmiller AM, White JA, Fang F 2nd, Wang X, et al. Amyloid precursor protein-mediated endocytic pathway disruption induces axonal dysfunction and neurodegeneration. J Clin Investig. 2016;126:1815–33.
44. Chen XQ, Zuo X, Becker A, Mobley WC. Hyperactivation of RAB5 disrupts the endosomal Rab cascade leading to endolysosomal dysregulation in Down syndrome: a necessary role for increased APP gene dose. Alzheimers Dement. 2025;21:e70046.
45. Kim S, Sato Y, Mohan PS, Peterhoff C, Pensalfini A, Rigoglioso A, et al. Evidence that the rab5 effector APPL1 mediates APP-betaCTF-induced dysfunction of endosomes in Down syndrome and Alzheimer's disease. Mol Psychiatry. 2016;21:707–16.
46. Kwart D, Gregg A, Scheckel C, Murphy EA, Paquet D, Duffield M, et al. A large panel of isogenic APP and PSEN1 mutant human iPSC neurons reveals shared endosomal abnormalities mediated by APP beta-CTFs, Not Abeta. Neuron. 2019;104:1022.
47. Lana-Elola E, Cater H, Watson-Scales S, Greenaway S, Muller-Winkler J, Gibbins D, et al. Comprehensive phenotypic analysis of the Dp1Tyb mouse strain reveals a broad range of Down syndrome-related phenotypes. Dis Model Mech. 2021;14:dmm049157.
48. Lana-Elola E, Watson-Scales S, Slender A, Gibbins D, Martineau A, Douglas C, et al. Genetic dissection of Down syndrome-associated congenital heart defects using a new mouse mapping panel. Elife. 2016;5:e11614.
49. Duchon A, Raveau M, Chevalier C, Nalesso V, Sharp AJ, Herault Y. Identification of the translocation breakpoints in the Ts65Dn and Ts1Cje mouse lines: relevance for modeling Down syndrome. Mamm Genome. 2011;22:674–84.
50. Pensalfini A, Kim S, Subbanna S, Bleiwas C, Goulbourne CN, Stavrides PH, et al. Endosomal dysfunction induced by directly overactivating Rab5 recapitulates prodromal and neurodegenerative features of Alzheimer's disease. Cell Rep. 2020;33:108420.
51. Zhu G, Zhai P, Liu J, Terzyan S, Li G, Zhang XC. Structural basis of Rab5-Rabaptin5 interaction in endocytosis. Nat Struct Mol Biol. 2004;11:975–83.
52. Hoffenberg S, Sanford JC, Liu S, Daniel DS, Tuvin M, Knoll BJ, et al. Biochemical and functional characterization of a recombinant GTPase, Rab5, and two of its mutants. J Biol Chem. 1995;270:5048–56.
53. Fellows AD, Rhymes ER, Gibbs KL, Greensmith L, Schiavo G. IGF1R regulates retrograde axonal transport of signalling endosomes in motor neurons. EMBO Rep. 2020;21:e49129.
54. Lalli G, Schiavo G. Analysis of retrograde transport in motor neurons reveals common endocytic carriers for tetanus toxin and neurotrophin receptor p75NTR. J Cell Biol. 2002;156:233–9.
55. Mitchell DJ, Blasier KR, Jeffery ED, Ross MW, Pullikuth AK, Suo D, et al. Trk activation of the ERK1/2 kinase pathway stimulates intermediate chain phosphorylation and recruits cytoplasmic dynein to signaling endosomes for retrograde axonal transport. J Neurosci. 2012;32:15495–510.
56. Sleigh JN, Villarroel-Campos D, Surana S, Wickenden T, Tong Y, Simkin RL, et al. Boosting peripheral BDNF rescues impaired in vivo axonal transport in CMT2D mice. JCI Insight. 2023;8:e157191.
57. Shekari A, Fahnestock M. Cholinergic neurodegeneration in Alzheimer disease mouse models. Handb Clin Neurol. 2021;182:191–209.
58. Lana-Elola E, Aoidi R, Llorian M, Gibbins D, Buechsenschuetz C, Bussi C, et al. Increased dosage of DYRK1A leads to congenital heart defects in a mouse model of Down syndrome. Sci Transl Med. 2024;16:eadd6883.
59. Borchers AC, Janz M, Schafer JH, Moeller A, Kummel D, Paululat A, et al. Regulatory sites in the Mon1-Ccz1 complex control Rab5 to Rab7 transition and endosome maturation. Proc Natl Acad Sci USA. 2023;120:e2303750120.
60. Hegedus K, Takats S, Boda A, Jipa A, Nagy P, Varga K, et al. The Ccz1-Mon1-Rab7 module and Rab5 control distinct steps of autophagy. Mol Biol Cell. 2016;27:3132–42.
61. Chen XQ, Zuo X, Becker A, Mante M, Florio JB, Jadhav SG, et al. Antisense oligonucleotides directed against App and Rab5 normalized endosomal Rab activity and reversed DS-AD-linked degenerative phenotypes in the Dp16 mouse model of Down syndrome. Alzheimers Dement. 2025;21:e70022.
62. Rhymes ER, Tosolini AP, Fellows AD, Mahy W, McDonald NQ, Schiavo G. Bimodal regulation of axonal transport by the GDNF-RET signalling axis in healthy and diseased motor neurons. Cell Death Dis. 2022;13:584.
63. Tosolini AP, Sleigh JN, Surana S, Rhymes ER, Cahalan SD, Schiavo G. BDNF-dependent modulation of axonal transport is selectively impaired in ALS. Acta Neuropathol Commun. 2022;10:121.
64. Vargas JNS, Brown A, Sun K, Hagemann C, Geary B, Villarroel-Campos D, et al. BDNF controls phosphorylation and transcriptional networks governing cytoskeleton organization and axonal regeneration. 2023. https://doi.org/10.1101/2023.11.06.565775.
65. Goto-Silva L, McShane MP, Salinas S, Kalaidzidis Y, Schiavo G, Zerial M. Retrograde transport of Akt by a neuronal Rab5-APPL1 endosome. Sci Rep. 2019;9:2433.
66. Fu X, Yang Y, Xu C, Niu Y, Chen T, Zhou Q, et al. Retrolinkin cooperates with endophilin A1 to mediate BDNF-TrkB early endocytic trafficking and signaling from early endosomes. Mol Biol Cell. 2011;22:3684–98.
67. Ramkumar A, Jong BY, Ori-McKenney KM. ReMAPping the microtubule landscape: how phosphorylation dictates the activities of microtubule-associated proteins. Dev Dyn. 2018;247:138–55.
68. Maday S, Twelvetrees AE, Moughamian AJ, Holzbaur EL. Axonal transport: cargo-specific mechanisms of motility and regulation. Neuron. 2014;84:292–309.
69. Baleriola J, Walker CA, Jean YY, Crary JF, Troy CM, Nagy PL, et al. Axonally synthesized ATF4 transmits a neurodegenerative signal across brain regions. Cell. 2014;158:1159–72.
70. Minis A, Dahary D, Manor O, Leshkowitz D, Pilpel Y, Yaron A. Subcellular transcriptomics-dissection of the mRNA composition in the axonal compartment of sensory neurons. Dev Neurobiol. 2014;74:365–81.
71. Villarin JM, McCurdy EP, Martinez JC, Hengst U. Local synthesis of dynein cofactors matches retrograde transport to acutely changing demands. Nat Commun. 2016;7:13865.
72. Qi Y, Liang Z, Wang Z, Lu G, Li G. Determination of Rab5 activity in the cell by effector pull-down assay. Methods Mol Biol. 2015;1298:259–70.
73. Schindelin J, Arganda-Carreras I, Frise E, Kaynig V, Longair M, Pietzsch T, et al. Fiji: an open-source platform for biological-image analysis. Nat Methods. 2012;9:676–82.
74. Tinevez JY, Perry N, Schindelin J, Hoopes GM, Reynolds GD, Laplantine E, et al. TrackMate: an open and extensible platform for single-particle tracking. Methods. 2017;115:80–90.

## ACKNOWLEDGEMENT

We thank the personnel of the MRC Prion Unit BSF for assistance in maintaining the mouse colonies. We thank Dr Sunaina Surana for help with purifying GST-tagged proteins.

## AUTHOR CONTRIBUTIONS

Conceptualisation: EB, OML, GS. Investigation: EB. Writing: Original Draft, EB; Editing: EB, NB, EMCF, OML, GS. Supervision: NB, EMCF, GS. Funding: EB, GS.

## FUNDING

This project was funded by the Eisai-Leonard Wolfson PhD Studentship to EB; Wellcome Investigator Awards (107116/Z/15/Z and 223022/Z/21/Z, GS); Medical Research Council grant (MR/T001976/1, OML and GS), MND Association Birsa/Oct21/976-799 (NB) and UK Dementia Research Institute (UKDRI-1005, GS), which receives its funding from UK DRI Ltd, funded by the UK Medical Research Council, Alzheimer's Society and Alzheimer's Research UK.

## COMPETING INTERESTS

The authors declare no competing interests.

## ETHICAL APPROVAL

All experiments were conducted under the guidelines of the UCL Genetic Manipulation and Ethics Committees and in accordance with the European Community Council Directive of 22 September 2010 (2010/63/EU).

## ADDITIONAL INFORMATION

**Supplementary information** The online version contains supplementary material available at https://doi.org/10.1038/s41419-026-08464-z.

**Correspondence** and requests for materials should be addressed to Giampietro Schiavo.

**Reprints and permission information** is available at http://www.nature.com/reprints

**Publisher's note** Springer Nature remains neutral with regard to jurisdictional claims in published maps and institutional affiliations.

**Open Access** This article is licensed under a Creative Commons Attribution 4.0 International License, which permits use, sharing, adaptation, distribution and reproduction in any medium or format, as long as you give appropriate credit to the original author(s) and the source, provide a link to the Creative Commons licence, and indicate if changes were made. The images or other third party material in this article are included in the article's Creative Commons licence, unless indicated otherwise in a credit line to the material. If material is not included in the article's Creative Commons licence and your intended use is not permitted by statutory regulation or exceeds the permitted use, you will need to obtain permission directly from the copyright holder. To view a copy of this licence, visit http://creativecommons.org/licenses/by/4.0/.

© The Author(s) 2026